A NUMERICAL ANALYSIS OF EXPERIMENTS ON MAGNETIC FIELD GENERATION

N. B. Volkov, V. T. Mikhkel'soo, and G. A. Shneerson

UDC 538.24.42

Introduction. A large number of papers, many of which were presented at the First and Second Conferences on Megagauss Fields [1], have been devoted to the investigation of the processes of hydrodynamic flow, diffusion of a magnetic field, and the evaporation of a surface in connection with magnetic field generation (MFG). The majority of the papers published have been devoted to the interpretation of individual experiments on flux compression by explosion or electromagnetic forces, and there have been practically no attempts (except the paper of Erber, et al. [2]) to analyze experiments over a wide range of parameters which permit solving the problem of what aspects of the process are the most decisive under the conditions of this or the other experiment.

One should note that such an analysis is possible only on the basis of a computational model which takes into account all aspects of the process, including the variation of conductivity at a phase transition, and which does not contain unjustified assumptions (thus, the generality of the analysis given in [2] is reduced due to the inclusion of characteristic quantities from experiments on MFG and the use of the concept of the skin-layer thickness, which is not always justified). Among the papers devoted to the investigation of individual physical factors, one should note the papers of Somon [3-5] (diffusion, compressibility, and liner instability), Brayant [6] (electrical explosion of the skin layer), and Lehner [7] (conductivity of a degenerate electron plasma). Only Kidder [8] and Kalitkin [9] have discussed the MFG process as a whole. Their discussions are not entirely satisfactory: Thus Kidder assumes the liquid–vapor phase transition to be discontinuous at temperatures above a critical temperature (T_{cr}), and Kalitkin assumes instantaneous expansion of the vapors to densities at which the expressions for the conductivity of a classical plasma are applicable, i.e., an instantaneous transition from metallic to plasma conductivity.

An analysis of MFG is made in this paper on the basis of a computational model of the interaction of a superstrong magnetic field with a metal in which a continuous transition from metal to plasma is taken into account (the latter is valid for processes in the course of which the dependence of the pressure p on the density does not intersect a binodal). An important assumption used below is the assumption of local thermodynamic equilibrium and the absence of explosions and macroscopic inhomogeneities everywhere in the medium except the boundaries of the region occupied by a conductor.

Computational Model. Here the metal is assumed to be a compressible conducting liquid. We shall neglect the distinction between the solid and liquid states, which is permissible when discussing the interaction of a superstrong field with a metal. The one-dimensional equations of motion of such a liquid are of the form

$$d\rho/dt + \rho\partial(rv)/r\partial r = 0; \tag{1}$$

$$\rho\frac{dv}{dt} = -\frac{\partial(p+q)}{\partial r} - \frac{B}{\mu_0}\frac{\partial B}{\partial r} + \frac{\partial S_{rr}}{\partial r} + \frac{S_{rr}-S_{\varphi\varphi}}{r}; \tag{2}$$

$$\frac{dB}{dt} = \frac{\partial}{r\partial r}\left(\nu r\frac{\partial B}{\partial r}\right) - B\frac{\partial(rv)}{r\partial r}; \tag{3}$$

$$\rho\frac{d\varepsilon}{dt} = -(p+q)\frac{\partial(rv)}{r\partial r} + S_{rr}\frac{\partial v}{\partial r} + S_{\varphi\varphi}\frac{v}{r} + \frac{\nu}{\mu_0}\left(\frac{\partial B}{\partial r}\right)^2 + \frac{\partial}{r\partial r}\left(\lambda r\frac{\partial T}{\partial r}\right), \tag{4}$$

where $d/dt = \partial/\partial r + v\partial/\partial r$ is the substationary derivative, $q = 0$ when $\partial v/\partial r \geq 0$ and $q = -a\rho(\partial v/\partial r)^2$ when $\partial v/\partial r < 0$ is the pseudoviscous pressure according to Neiman–Richtmyer [10], which is introduced for the computer calculation of shock discontinuities, $\mathbf{S}$ is the tensor of the tangential stresses, which is assumed here to be viscous, $\nu = (\mu_0\sigma)^{-1}$ is the magnetic viscosity, and p, ε, σ and λ are the pressure, internal energy, electric conductivity, and electron thermal conductivity of the metal, respectively.

Istra. Translated from Zhurnal Prikladnoi Mekhaniki Tekhnicheskoi Fiziki, No. 5, pp. 15-26, September-October, 1982. Original article submitted July 21, 1981.

0021-8944/82/2305-0607$07.50

We note that the introduction of the tangential stress tensor into the computational model is not obligatory, since in fields with induction B > 3 MG a metal behaves like an ideal liquid [11]. It is introduced here in order to avoid singularities on the free boundaries of a metal, where its density may become equal to zero. Therefore at $r = r_e$ and $r = r_i$ (the subscripts "e" and "i" refer to the exterior and interior liner boundaries, respectively)

$$(S_{rr} - p)_{e,i} = \begin{cases} 0, & \sigma \neq \infty, \\ B^2/2\mu_0, & \sigma = \infty. \end{cases}$$

In addition at $r = r_{e,i}$ $dr_{e,i}/dt = v_{e,i}$. It has been assumed that there is no heat exchange with the surroundings. Then

$$\partial T/\partial r|_{r_{e,i}} = 0.$$

The boundary conditions for the field are determined by the transition process in the external electric circuit or are specified in the form of some function of the time. In the case of a liner which has collapsed to the axis, it is necessary that the law of electromagnetic induction

$$d\Phi_0/dt = 2\pi r_i v_i (\partial B/\partial r)_{r=r_i},$$

be satisfied on the interior boundary, where Φ_0 is the flux in the liner cavity. On the exterior boundary of the liner $(\partial B/\partial r)r_e = 0$ or the field is specified by some function of time which determines the transition process in the external electric circuit.

If the liner is accelerated by electromagnetic forces (magnetodynamic field generation (MDFG)), then it is necessary to take account of the edge effects associated with the finite length of the liner [12, 13] in the boundary conditions. On the basis of the superposition principle and the law of total flux, one can write them in the form [14, 15]

$$\begin{aligned} B_e &= B_0 + \mu_0[I_s K_1(r_i) + K_2(r_i) I_0]/l, \\ B_i &= B_0 + \mu_0[K_3(r_i) I_s - K_4(r_i) I_0]/l, \\ B_s &= B_0 + \mu_0[K_5(r_i) I_s - K_6(r_i) I_0]/l, \\ \Phi_0 &= M(r_i) I_s = L_0(r_i) I_0, \end{aligned}$$

where B_S is the induction on the liner axis, I_S and I_0 are the currents in the solenoid and the liner, respectively, and $K_1(r_i) - K_6(r_i)$, $M(r_i)$, $L_0(r_i)$ are dimensionless coefficients and the mutual and self-inductances of the liner, which are determined either by physical modeling similarly to [15] or by computational means under conditions of a sharply expressed skin effect.

The initial conditions have different forms in the case of MFG and MDFG. For MFG at time $t = 0$, $v_i = v_0$, $v(r) = v_i r_i/r$, $\rho = \rho_0$, $B = B_0$, $T = T_0$, $r_i = r_0$, and $r_e = r_0 + h_0$. For MDFG the motion of the shell is considered from the start of the acceleration; one can assume the shell material to be incompressible, and it is necessary in addition to specify the parameters of the accelerating contour.

Equations (1)-(4) along with the initial and boundary conditions are reduced to dimensionless form, discretized on a Lagrangian grid, and numerically solved by the forcing method. Nonuniform partition into layers is provided for in the algorithm with the goal of the best exposure of the skin-layer structure. In the case of MDFG such a rearrangement is made twice: At the start of the process and after the current in the liner passes through zero, when the field on the interior boundary becomes greater than that on the exterior boundary. The integration step is variable and is calculated from the condition

$$\tau \max_i \{[c_i^2 + B_i^2/\mu_0\rho_i]^{1/2}/\Delta_i r\} \leqslant 1,$$

where $i = 1, 2, \ldots, N-1$, $\Delta_i r = r_i - r_{i-1}$, and c_i and $B_i/(\mu_0\rho_i)^{1/2}$ are the local speed of sound and the Alfven velocity, respectively. A solution algorithm along with the formulation of the problem of magnetic flux compression by a conducting liner have been described in [16].

When solving Eqs. (1)-(4) the three-term equations of state

$$p(\rho, T) = p_x(\rho) + p_T(\rho, T) + p_{Te}(\rho, T); \tag{5}$$

$$\varepsilon(\rho, T) = \varepsilon_x(\rho) + \varepsilon_T(\rho, T) + \varepsilon_{Te}(\rho, T), \tag{6}$$

were used, where [17]

$$p_x(\rho) = c_0^2 \rho_0 \delta^2 (\delta - 1); \tag{7}$$

$$\varepsilon_x(\rho) = 0.5 c_0^2 (\delta - 1)^2 \tag{8}$$

describe the contribution of the motion of electrons at $T=0$ to the pressure and the energy ((7) and (9) are valid for $p \leq 10^{12}$ Pa; c_0 is the speed of sound in an unperturbed metal, and $\delta=\rho/\rho_0$ is the relative density), [18] $\varepsilon_T(\rho, T)=C_V(\rho, T)T$, and $p_T(\rho, T)=\Gamma(\rho, T)\rho\varepsilon_T(\rho, T)$ describe the contribution of the thermal motion of ions to the energy and pressure, [18] $\varepsilon_{Te}(\rho, T)=b^2 \ln\cosh(\beta T/b)$, and $p_{Te}(\rho, T)=2\rho\varepsilon_{Te}(\rho, T)/3$ describe the contribution of the thermal excitation of the conductivity electrons to the energy and pressure; $C_V=[1+0.5\xi_1(\rho, T)]C_\rho/[1+\xi_1(\rho, T)]$ ($C_\rho=3Nk$ is the specific heat of the metal), $\xi_1(\rho, T)=l_1C_\rho T/3(dp_x/d\rho-2n_1p_x/3\rho)$; n_1 and l_1 are constants defined by the authors of [18] on the basis of experiments on shock compression of porous metals (one can also determine them if one knows the critical parameters), $\beta=\beta_0\delta^{-2/3}$, and $\beta_0=4\pi^{-4}k^2mh^{-2}N_e^{1/3}(3\pi^2\rho_0)^{-2/3}$ [11] (N_e is the number of free electrons in 1 kg of the metal; for copper $n_1=0$, $l_1=9.25$, $b=5.6\times10^3$ J/kg·°K, and $\beta_0=1.09\times10^{-2}$ J/kg·°K^2). Thus the selected equations of state satisfy the known asymptotes for $\delta=0$, $\delta=1$, $\delta=\delta_S$, $p=p_S$, and $T=T_S$, and also as $T\to\infty$, and consequently they describe a continuous transition in the supercritical region from a metal to a plasma.

It is well known [19] that the Weidman–Franz law $\lambda=9k^2T\sigma/\pi e^2$ is valid for the electron thermal conductivity of a metal. In the region of plasma densities, $\lambda\sim2k^2T\sigma/e^2$, as has been shown in [9]; therefore one can approximately use the Weidman–Franz law to estimate λ over the entire range of variation of T and p.

The tangential stress tensor is a viscous tensor, which in a Cartesian coordinate system has the form [20]

$$S_{ik}=\eta\left(\frac{\partial v_i}{\partial x_k}+\frac{\partial v_k}{\partial x_i}-\frac{2}{3}\delta_{ik}\frac{\partial v_j}{\partial x_j}\right), \tag{9}$$

where $\delta_{ik}=0$ if $i\neq k$, $\delta_{ik}=1$ if $i=k$, and η is the viscosity coefficient. Since (9) is introduced in order to avoid singularities on the free boundaries of the liner; we shall assume η to be constant and small in order that the required condition be provided.

Both the approximation [21]

$$\sigma=\sigma_0\delta^{\xi}/1[1+\beta_TC_V(T-T_0)] \tag{10}$$

(ξ is the pressure drag coefficient, β_T is the thermal drag coefficient, and σ_0 is the value of σ at $T=300$°K) and the expression derived in [22] upon taking phenomenological account of the peculiarities of electron scattering in a metal and a plasma:

$$\sigma=16\pi\varepsilon_0^2\langle W_k\rangle^{3/2}\varkappa/(\sqrt{2m}e^2Z\Lambda nkT), \tag{11}$$

where $\langle W_k\rangle$ is the average kinetic energy of the electrons, $\varkappa=\rho(\partial p/\partial\rho)_T$ is the modulus of isothermal compressibility, $\Lambda=\ln(1+\zeta)-\zeta/(1+\zeta)$ is the analogue of the Coulomb logarithm, $\zeta=16m\langle W_k\rangle^2/Z^2e^2\hbar^2n$, and n is the average concentration of ions (also see [23], where a more exact expression has been obtained for the conductivity), are used here as the conductivity. We note that (11) differs only by the factor $2\varkappa/\Lambda nkT$ from the formula of Lehner [7], which provides the correct asymptotes for $T<T_F$ and $T>T_F$ ($T_F=\varepsilon_F/k$ is the Fermi temperature, and ε_F is the Fermi energy). In order to find $\langle W_k\rangle$ and $\varkappa$, we shall use Equations (5) and (6):

$$\sigma=0.054F^{3/2}\varkappa/\Lambda T\ \Omega\text{m}\cdot\text{m})^{-1}; \tag{12}$$

$$\zeta=0.69\cdot10^{-8}(\rho_0/AMZ)^{1/3}\delta^{1/3}F; \tag{13}$$

$$F=\langle W_k\rangle\varepsilon_F^{-1}=1+5.9\cdot10^{14}(AM/Z\rho_0)^{2/3}\ b\ \text{lnch}(\beta T/b)/\beta_0 \tag{14}$$

(A, M, and Z are the atomic weights, unit of mass, and charge of the nucleus, respectively; [M], [ρ], [$\varkappa$], and [T] are measured in the SI system in (12)-(14). At $T=300$°K and $\delta=1$ (12)-(14) give a value of $2.75\times10^{-8}\ \Omega\cdot$m for the specific resistance of copper. A comparison of the values of σ from (12)-(14) with the known experimental data and calculations based on the Boltzmann equation shows justification for using the expressions (12)-(14) to interpret the experiments on MFG (the fact that Z is assumed to be constant in (12)-(14) does not introduce a large error into the MFG conditions [22], as the calculations show).

A Powerful MHD Shock Wave in a Conducting Half-Space. In this section we shall discuss the propagation of a powerful MHD shock wave (SW) into a half-space, which permits comparing different models and investigating the general characteristics of the interaction of a metal with a superstrong field. The axisymmetric problem was solved; the interior radius of the cylinder was taken to be such that the SW did not differ greatly from a plane wave (it is equal to 40 cm here). The field on the interior boundary was specified in the form $B(t)=B_m(1-\exp(-t/\tau)$, and B_m took the values 300, 500, 700, 10^3, and 1.5×10^3 T. The value of the time constant for all B_m is equal to 0.3 μsec (the choice of such a value was determined by the characteristic rise time of the field pulse at the end of MFG).

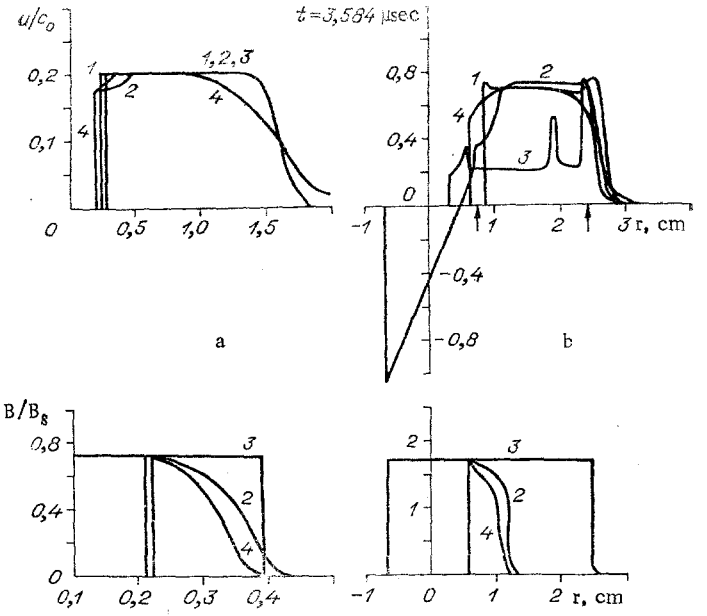

Fig. 1

TABLE 1

Model	B, MG / u/c_0	3	5	7	10	15	Metal
1	u_i/c_0	0,205	0,446	0,708	1,118[1)]	1,821[2)]	
	u_f/c_0	0,171	0,444	0,644	1,144	1,867	
2	u_i/c_0	0,182	−0,372[3)]	−1,2	−2,369	−4,359	
	u_f/c_0	0,198	0,459	0,759	1,1	1,808	
	u_s/c_0	0,205	0,454	0,721	1,16	1,841	
3	u_i/c_0	0,168	0,216	0,175	0,256	0,308	
	u_f/c_0	0,197	0,418	0,733	0,405	0,838	
	u_p/c_0	0,19	0,444	0,708	0,859	0,838	
	u_s/c_0	0,206	0,444	0,708	0,859	0,838	
4	u_i/c_0	0,183	0,285	0,544	1,031	1,831	
	u_f/c_0	0,199	0,438	0,679	1,072	1,769	
	u_s/c_0	0,202	0,446	0,703	1,108	1,831	
1	u_i/c_0	0,176	0,384	0,622	0,98	1,611	
	u_f/c_0	0,167	0,362	0,627	0,962	1,58	
2	u_i/c_0	0,109	−0,21	−1,033	−1,622	−2,933	
	u_f/c_0	0,179	0,413	0,7	1,038	1,8	Stainless steel
	u_s/c_0	0,172	0,411	0,7	1,089	1,789	4) t=2,22 μsec; the rest,
3	u_i/c_0	0,172	0,157	0,186	0,195	0,198[4)]	t=3,6 μsec.
	u_f/c_0	0,165	0,165	0,148	0,393	0,269	
	u_p/c_0	0,177	0,349	0,424	0,393	0,269	
	u_s/c_0	0,177	0,349	0,424	0,393	0,269	

The results of calculations illustrating the application of the computational model and a comparison of them with the results obtained from other models are presented in Fig. 1 and in Table 1 (the following notation is used in Fig. 1: 1) ideally conducting medium; 2) formula (10) is used as σ; 3) idealized explosion of the skin layer (it is assumed in this model that when $T < T_S$ σ is determined by (10) and when $T \geq T_S$ $\sigma = 0$); and 4) the plasma model of the conductivity; σ is determined by (12)-(14); the subscripts "a" and "b" correspond to fields of 3 and 7 MG, respectively). The velocities of the interior boundary (u_i), the SW front (u_f), the field−conductor boundary (u_p), and the current front (u_s) for copper and stainless steel are presented in Table 1.

The results of Table 1 and Fig. 1 show that when there is no electrical explosion of the skin layer all the models give practically identical descriptions of the shock front. When $B \geq B_S = (\mu_0 \rho_0)^{1/2} c_0$ (B_S defines the

limit above which the energy entering the conductor is greater than the sublimation energy), an electrical explosion of the skin layer is possible. As Fig. 1 shows, when $B = 300$ T ($0.726B_S$ for copper and $0.658B_S$ for steel), an idealized explosion has no effect on the value of the velocity of the field–conductor boundary, which is close to the velocity of the interior boundary of an ideal conductor (see Table 1); the thickness of the evaporating layer does not exceed the thickness of the skin layer ($\lesssim 1$ mm). The results of computations using (10) show (Fig. 1) that in fields greater than B_S the velocity of the interior boundary changes sign due to a rarefaction wave, which causes a negative pressure gradient on the SW front and the impossibility of the magnetic field preventing the expansion of weakly conducting layers of the metal (curve 2, Fig. 1b). The boundary of the current front is located far from the boundary (the first arrow from the origin of coordinates). Since the magnetic pressure at this location is a maximum, a small maximum is observed on the velocity curve (curve 2, Fig. 1b). The density of the metal layers with a negative velocity is much less than the initial density ($\delta = \rho/\rho_0 \lesssim 0.1$; $\delta \sim 0.1$ corresponds to the effective field–conductor boundary), and the conductivity is close to zero. If one neglects the mass of the expanding layers and uses formula (10) as σ in the remainder, then one can describe rather accurately the motion of the effective field–conductor boundary (this approach corresponds to Brayant's hypothesis [6] that the conductivity disappears with a discontinuity at $\delta = 0.1$). Such a viewpoint has been used in [14, 16] in the investigation of MFG. A comparison of the computational results obtained using (10) and (12)-(14) with each other shows the validity of this viewpoint, since the latter model gives an effective cutoff of the density at the $\delta \sim 1$ level (see curve 4, Fig. 1b). The thickness of the skin layer is somewhat less than for the model using (10). This circumstance is caused by the more accurate description of the $\sigma(\rho)$ dependence by the expressions (12)-(14).

In fields larger than B_S an idealized explosion of the skin layer occurs on the SW front (the second arrow on Fig. 1b). Irregularities in the velocity curve are related to nonconducting vapor and are caused by the presence in it of compression and rarefaction waves. The phase velocity of the field–conductor boundary is equal in this case to the magnetosonic velocity $v_p = (c^2 + v_A^2)^{1/2}$ ($c = ((\partial p/\partial \rho)_T)^{1/2}$ and $v_A = B/(\mu_0 \rho)^{1/2}$ are the sound and Alfvén velocities, respectively). When there is no explosion of the skin layer, the effective velocity of the field–conductor boundary is well approximated by the expression $v_p = 0.5 c_0 \lambda_1^{-1}[(1 + 2\lambda_1 v_A^2/c_0^2)^{1/2} - 1]$ (λ_1 is an empirical constant of the metal).

The model of an idealized explosion of the skin layer is of a formal nature; therefore, one can only speak of its absence or inappreciable influence on the rate of movement of the field–conductor boundary for copper and steel when $B \leq 4$ MG. One can apply it to find the limiting characteristics of MHD flows of a metal in a superstrong field. This model is applied below to interpret experiments on MFG in fields stronger than 5 MG: It is shown that at least in the case of conductors of the stainless steel type this model is not devoid of physical meaning.

Since an unloading wave arises even in the case of a field of the form $B(t) = B_m(1 - \exp(-t/\tau))$, conditions for its onset are investigated for MFG, where the lifetime of the shell determines the duration of the field pulse [14]. The field was varied in the calculation according to the law $B(t) = A(\exp(-t/\tau_1 - \exp(-t/\tau_2))$ (τ_1 and τ_2 are chosen to be equal to the characteristic values for actual field pulses obtained in MFG; the maximum values of the field are equal to 3.26, 6.38, and 12.6 MG). As a result of calculations using the plasma model of conductivity (expressions (12)-(14)), the following picture of the onset of a rarefaction wave is revealed. At time $t = t_m$, when the field becomes a maximum, the velocity of the interior boundary (v_i) changes to the opposite sign (until $t = t_m v_i > 0$) under the action of a negative gradient of the hydrodynamic pressure (in MFG the pressure gradient in the liner wall is always negative). A decrease of the field on the interior boundary results in the fact that its maximum appears in the interior of the shell wall due to the inertia of the magnetic flux. A negative gradient of the magnetic pressure also leads to an increase in the velocity of the interior boundary ($v_i < 0$).

In MFG the velocity of the interior boundary of the shell is always less than zero; in addition the maximum of the field occurs before its complete halting due to the finite value of σ. Therefore the occurrence of an additional velocity due to a rarefaction wave which coincides in direction with the shell velocity can result in its destruction. If the conductivity of the inner layers is large, the shell will not be destroyed but will stop at a radius smaller than the dimensions of the inductive detector or the object of the investigations (it is shown below that this has occurred in a number of experiments).

Analysis of Experiments on Magnetic Field Generation. The models discussed above are used to interpret experiments on MFG and MDFG. Experiments performed at the M. I. Kalinin Leningrad Polytechnic Institute are taken as the latter (the interpretation of the experiments of other authors requires knowledge of the parameters of their accelerating contours, which is not always possible). These experiments are character-

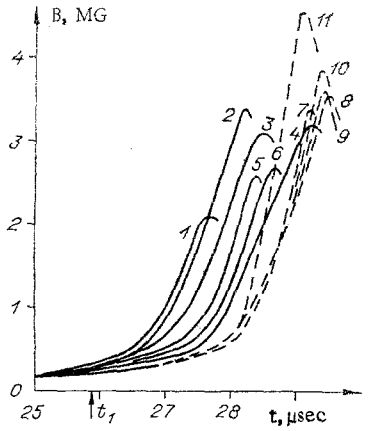

Fig. 2

ized by care with the experimental conditions, which permitted obtaining a record value of the induction for MDFG (B_m = 3.4 MG). Those experiments in which reproducible values of B_m were obtained are taken from experiments in which the liners were accelerated by an explosion, which indicates symmetry of compression of the liner.

Calculation of MDFG was performed together with the acceleration stage of the liner; the computational results for this stage are in good agreement with experiment. Thus in a series of experiments with liners made out of copper with diameter d_0 = 45 mm and thickness h_0 = 0.38-0.41 mm the experimental magnetic flux captured by the liner was $\Phi_1 = 2 \pm 0.4$ mWb and the calculated value was Φ_1 = 1.68-1.87 mWb; the experimental conversion coefficient of contour energy into kinetic energy of the shell was η = 6.8-7.8%, and the calculated value was η = 6.91-7.3%. The experimental time at which the current in the liner passed through was t_1 = 25.9 μsec, and the calculated value was 25.96 μsec.

Figure 2 contains the results of MDFG experiments (solid curves) of copper liners with d_0 = 45 mm and h_0 = 0.38-0.41 mm and the results of calculations (dashed curves) for a shell with h_0 = 0.4 mm (the computational results for other thicknesses and radii are given in generalized form on the diagram of Fig. 6). The curves of Fig. 2 were obtained using the models: 7) ρ = var, $\sigma \neq \infty$; the contributions of p_x and p_x and p_T are taken into account in the equation of state, and in addition the possibility of accomplishing an idealized explosion of the skin layer is provided for; 8) ρ = var, $\sigma \neq \infty$; only p_x is taken into account in the equation of state; 9) ρ = var; $\sigma = \infty$; 10) $\rho = \rho_0$ = const, $\sigma \neq \infty$; and 11) $\rho = \rho_0$ = const, $\sigma = \infty$. The calculated curves of Fig. 2 lie in a dense bunch of experimental curves between which the temporal discrepancy and the difference in the value of B_m were caused by the difference in shell thicknesses and experimental conditions. The maximum value B_m = 3.4 MG corresponds to the experiment with h_0 = 0.4 mm. The best agreement with this experiment is given by the most complete model (curve 7) – B_m = 3.35 MG. The temporal shift between the calculated and experimental maxima, which is equal to 1 μsec, does not exceed the measurement error and is much less than the duration of the entire process, which is equal to 29 μsec. The value of the calculated radius of reverse behavior r_m (the minimum radius, after attainment of which the shell should in principle expand) was less than the experimental value (the experimental value of r_m according to estimates of [13] based on SFR-grams was 2 mm, and the calculated value was 0.925 mm, which is larger than the probe radius, which is equal to 0.8 mm).

Let us consider the relative contribution of each of the physical factors to B_m and r_m. We have (the subscripts "0", "d", and "c" refer respectively to a liner without losses, an incompressible liner with $\sigma \neq \infty$, and a compressible liner with $\sigma = \infty$) $B_{m0}/B_{md} = 1.158$, $B_{m0}/B_{mc} = 1.239$, $B_{md}/B_{mc} = 1.07$, and $B_{m0}/B_m = 1.253$ – a one-term equation of state and $B_{m0}/B_m = 1.331$ – a two-term equation of state. Consequently, $r_{m0}/r_{md} = 1.552$, $r_{m0}/r_{mc} = 0.902$, $r_{m0}/r_m = 1.293$, $r_{m0}/r_m = 1.297$, $\Phi_1/\Phi_{md} = 2.779$, $\Phi_1/\Phi_m = 1.961$, and $\Phi_1/\Phi_m = 1.968$. Analysis of the cited figures indicates that in these experiments compressibility was the determining factor, and diffusion introduces corrections to B_m (compressibility decreases the flux losses). Since both factors have a different effect on r_m, B_{md} differs somewhat from B_{mc}. This "restoring" role of diffusion in experiments in which the thickness of the skin layer $\Delta < r_m$ has been noted in [14]. These experiments show that the most sensitive parameter to the choice of physical model is the radius of reverse behavior, which is unfortunately not recorded in the majority of MFG experiments. Figure 2 also shows that there is no electrical explosion of the skin layer in the experiments of [13]. Analysis of experiments with liners of larger diameters and made out of various materials has shown that one should refer experiments with liners of larger

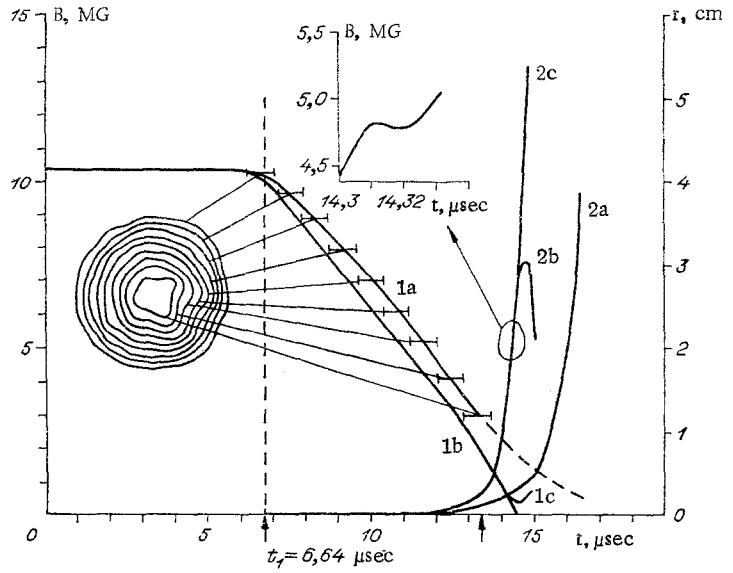

Fig. 3

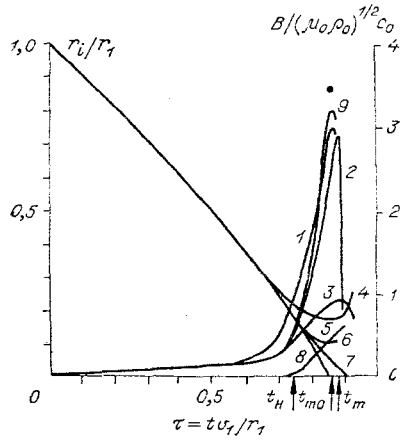

Fig. 4

diameter to the case of ideal cumulation, when the compressibility and diffusion due to the large value of the captured flux have practically no effect on B_m and r_m; compressibility plays a larger role for shells made out of aluminum than in the case of copper or brass shells.

The results of an experiment [24] with a liner made out of stainless steel, in which B_m = 9.8 MG, and of a calculation are shown in Fig. 3 (in Fig. 3 the labels are as follows: 1) $r_i(t)$; 2) $B(t)$). Calculation using the approximation (10) has given a highly exaggerated value of the induction for a practically zero radius of reverse behavior (curves 2a and 1b). A calculation which uses the model of an idealized explosion of the skin layer gave B_m = 8 MG (curve 2b) with r_m larger than the probe radius. The calculated $B(t)$ curve has a step at the onset time of the electrical explosion; therefore if there is an electrical explosion of the skin layer which is close to an idealized one, then one can detect it from the sharp bend of the experimental $B(t)$ curve. Since in the case of MFG with liners made out of poor conductors the thickness of the skin layer is much greater than the radius of reverse behavior, B_m is determined by the effective radius $r_{eff} \sim \Delta$. The action of an idealized explosion therefore reduces to dropping from the discussion layers of metal which have in fact lost conductivity (this situation is accomplished in a self-consistent manner in the MHD calculations). We note that the calculated liner radius is in good agreement with the experimental value (curves 1a and 1b, Fig. 3) in the region accessible to measurement.

Figures 4 and 5 show the results of the experiment of Fowler with his co-workers [25], in which B_m = 14.3 MG, and of a calculation using different models (the following notation is adopted in Fig. 4: $B(t)$: 1) $\sigma = \infty$; 2) $\sigma \neq \infty$, explosion after maximum field; 3) $\sigma \neq \infty$, idealized explosion; and 9) plasma model of the conductivity; the experimental value of B_m is denoted by the filled circle; $r(t)$: 4) field–conductor boundary for an idealized explosion; 5) additional shift of the field–conductor boundary due to an explosion; 6) $\sigma = \infty$; 7) $\sigma \neq \infty$, no explosion; and 8) interior boundary of the nonconducting vapor). Figure 4 shows that, notwithstanding the fact that

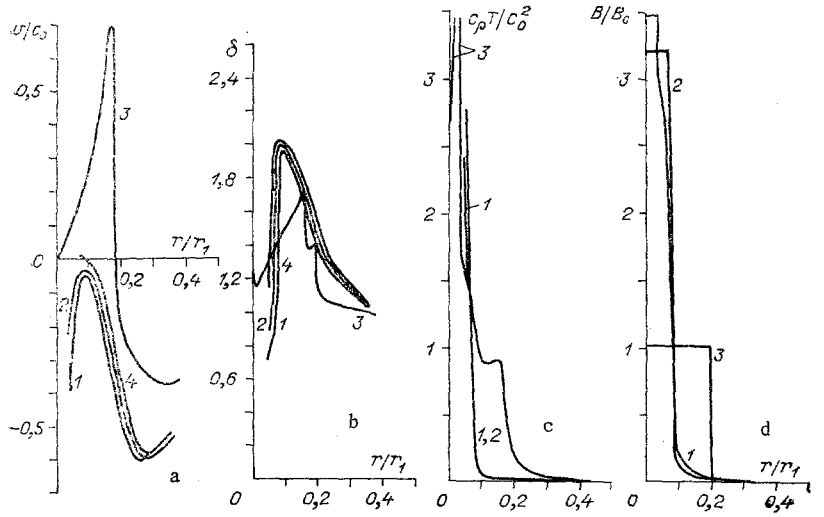

Fig. 5

the approximation (10) is used outside the region of its applicability, the computational results are in good agreement with experiment (curve 2). The later is explained by the fact that, as has been shown in the preceding section, the expression (10) satisfactorily describes the shock front as well as the parameters of the current front if one neglects the ejection of metal due to loss of conductivity as a discontinuity when $\delta \leq 0.1$. Taking account of the thermal components in the equation of state results in a decrease of r_m, as the calculations show. The plasma model of conductivity (curve 9 of Fig. 4) gives still better agreement with experiment (difference of 7.7%). The model of an idealized explosion (curve 3, Fig. 4) results in an abrupt decrease of B_m in comparison with experiment, which permits concluding that it is not present in experiments with copper and brass shells. The effective field–conductor boundary and its phase velocity are practically constant (the latter $\sim c_0$; see curve 5 in Fig. 4, which shows an additional shift of the field–conductor boundary as a result of the explosion).

Comparison of the calculation with $\sigma = \infty$ with the analytic estimates for a shell without losses and a compressible shell with $\sigma = \infty$ shows that in the experiment of [25] the effect of compressibility and diffusion is weakly expressed; more exactly, the mutual action of these factors leads to a situation in which the maximum field is achieved at $t = t_{m0}$ (plasma model) at a somewhat smaller radius than r_{m0}. As a calculation using the plasma model shows, the maximum value of the specific resistance which corresponds to the maximum field, is located inside the liner wall. The latter situation results in a decrease of the magnetic flux losses from the liner cavity (this was also noted in [9]). This decrease is still more noticeable in experiments of the type of the experiment of [26], in which compressibility played the determining role.

Actually, using the estimate of the limiting value of the induction B_∞ [27]

$$B_\infty = B_c \left[\frac{2v_1}{c_0} \left(1 + \lambda_1 \frac{v_1}{c_0} \right) \right]^{1/2} \tag{15}$$

(λ_1 is an empirical characteristic of the metal [11]; for copper $\lambda_1 = 1.5$), we obtain, having taken $v_1 = 11.8$ km/sec, $B_\infty = 23.8$ MG on the basis of a calculation [9], the following results: the calculation of [9] – $B_m = 30$ MG, our calculation – $B_m = 22.4$ MG, and experiment – $B_m = 25$ MG; the calculated radius on reverse behavior is 2 mm. The results obtained permit concluding that in very strong fields ($B \geq 10$ MG) an electrical explosion of the skin layer is evidently not observed in principle, and MFG is limited by the compressibility of the metal and by instabilities.

Due to this one can give an additional argument. An estimate is obtained in [14] for the effect of diffusion in the case of good conductors namely

$$B_{md} = B_{m0}(r_{m0} + 2\Delta)/(r_{m0} + 2.5\Delta), \tag{16}$$

where Δ is the thickness of the skin layer, which is determined by the expression [14]:

$$\Delta = 0.655 r_{m0} (\Lambda \rho_0/\mu_0)^{1/4} (B_{m0}/r_{m0}\sigma_0 B_1^2)^{1/2}; \tag{17}$$

$\Lambda = \ln(1 + s_0/\pi r_{m0}^2)$; s_0 is the cross sectional area of the shell, and σ_0 and B_1 are the initial values of the electrical conductivity and the magnetic field, respectively. Let us consider a hypothetical incompressible shell for

which $r_{m0} = r_{mc}$ and $B_{m0} = B_{mc}$. Then one can approximately estimate from formulas (16) and (17) the combined effect of diffusion of the magnetic field and compressibility. In this case the ratio Δ_s/r_{mc} (Δ_s is the thickness of the skin layer in a compressible shell) will be determined by the expression

$$\Delta_s/r_{mc} = (\Delta/r_{m0})(B_{mc}/B_{m0})^{1/2}.$$

Since an increase in the compressibility results in a decrease in B_{mc}, when $B_{m0} \gg B_{mc}$ and $\Delta_s/r_{mc} \ll \Delta/r_{m0}$, i.e., in the limit of infinitely large B_{m0} (large v_1 or small B_1) $B_m \to B_{mc} \to B_\infty$.

Let us return again to the experiment of [25]. The distribution of the velocity, density, temperature, and field through the liner thickness at the time of maximum field is shown in Figs. 5a-d, respectively, for a liner with $\sigma = \infty$ (curve 4), the model of an idealized explosion (curve 3), the plasma model of conductivity (curve 2), and a calculation using (10) (curve 1). A comparison of curves 1 and 2 with curve 4 shows that at the time of maximum field the velocity of the interior liner layers is not equal to zero but increases towards the interior boundary, which is associated with the nature of the density distribution (curves 1, 2, and 4 of Fig. 5b) and the finite value of σ. Such behavior of the velocity and density actually confirms the possibility of the onset of a rarefaction wave discussed in the preceding section, which can lead to a decrease in the lifetime of the liner, and consequently a decrease in the effective duration of the field pulse. Calculation has shown that in this particular case halting of the shell has nevertheless occurred (Fig. 4); in the case of liners made out of poor conductors there is no such halting, as has been mentioned above, or it occurs at a radius less than the probe radius. Practically all the published experiments on MFG are presented in Fig. 6. These experiments have been previously discussed in detail in [28, 29], where the radius of reverse behavior is identified with the probe radius. Here this assumption is refined: As the calculations have shown, all experiments on MFG are divided into two groups — "good," in which the liner did not fly onto the probe, and "bad," in which the opposite situation occurred (they are shown on the left and the right, respectively, in the diagram). The diagram shows that one should attribute a large part of the experiments to the "bad" group since exaggerated values of the induction amplitude are obtained in them due to the large diameter of the probes (for example, in experiment LA-2 according to Herlach's classification $B_m = 4$ MG is obtained, and in calculation using the idealized explosion model $B_m = 10.1$ MG for $r_m = 1.3$ mm; a simple recalculation for a probe radius $r_p = 1.6$-2.75 mm gives $B_m = 2.26$-6.67 MG).

The analysis carried out above and Fig. 6 permit formulating the main result of this paper: All experiments on MFG are divided into four classes: 1) $B_m \leq 2$ MG — ideal cumulation; 2) $2 \leq B_m \leq 4$ MG $\sim B_c$ — cumulation close to ideal (diffusion of the magnetic field and compressibility play a weak role); 3) 4 MG $\sim B_c \leq B_m \leq$ 10 MG — flux losses and electrical explosion of the skin layer determine B_m (all experiments with liners made out of stainless steel fall into this range). Since the temperature of the vapors formed is insufficient for their

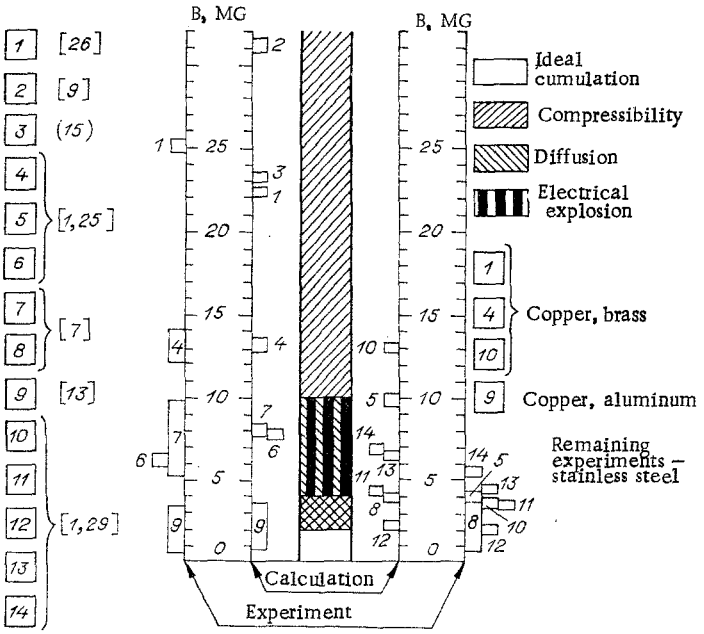

Fig. 6

ionization, the model of an idealized explosion of the skin layer, which gives a lower limit of the induction produced and an upper limit of the radius of reverse behavior, can be a good approximation for the investigation of the compression of flux by shells made out of stainless steel or similar conductors; and 4) $B_m > 10$ MG — experiments in which for observance of symmetry of liner compression B_m is determined by the compressibility, there is no electrical explosion of the skin layer, and diffusion of the field is of a corrective nature; for copper and similar conductors, starting from $M = v_1/c_0 \geq 3$, a good estimate of the induction amplitude is B_∞ defined by the expression (15).

A more accurate criterion of the correctness of the computational models discussed here would be a comparison with experiment of the value of the reverse behavior radius, for which there are no reliable experimental data. It is possible that a more careful analysis will show the limited nature of the models discussed here, which do not take account of kinetic effects and macroscopic inhomogeneities of the medium.

In conclusion the authors consider it their responsibility to express their gratitude to E. I. Bichenkov, V. S. Imshennik, and N. N. Kalitkin for their interest in the research and for useful discussions.

LITERATURE CITED

1. H. Knoepfel and F. Herlach, in: Proceedings of the Conference on Megagauss Magnetic Field Generation by Explosives and Related Experiments, Euratom, Brussels (1966); H. Knoepfel and F. Herlach, in: Second International Conference on Megagauss Magnetic Field Generation and Related Topics, Washington, D.C. (1979).
2. T. Erber, H. G. Latal, et al., "Analysis of flux compression experiments," Acta Phys. Austr., 36, 171, 257, and 316 (1972).
3. J. P. Somon, "Magnetic fields obtained by flux compression. Limitation due to diffusion of the cylindrical liner," in: Proceedings of the Conference on Megagauss Magnetic Field Generation by Explosives and Related Experiments, Euratom, Brussels (1966).
4. J. P. Somon, "Magnetic fields obtained by flux compression. Limitation due to dynamics of the cylindrical liner," in: Proceedings of the Conference on Megagauss Magnetic Field Generation by Explosives and Related Experiments, Euratom, Brussels (1966).
5. J. P. Somon, "The dynamical instabilities of cylindrical shells," J. Fluid Mech., 38, 769 (1969).
6. A. R. Brayant, "The effect of Joule heating on the diffusion of megagauss fields," in: Proceedings of the Conference on Megagauss Magnetic Field Generation by Explosives and Related Experiments, Euratom, Brussels (1966).
7. G. Lehner, "The limits on production of very strong magnetic fields," Springer Tracts in Modern Physics, 47, 67 (1965).
8. R. E. Kidder, "Compression of the magnetic field inside a hollow explosive-driven cylindrical conductor," in: Proceedings of the Conference on Megagauss Magnetic Field Generation by Explosives and Related Experiments, Euratom, Brussels (1966).
9. N. N. Kalitkin, "Materials at high energies," Author's Abstract of Doctoral Dissertation, Physicomathematical Sciences, IPM Akad. Nauk SSSR, Moscow (1972).
10. R. Richtmyer and K. Morton, Difference Methods for the Solution of Boundary-Value Problems [Russian translation], Mir, Moscow (1972).
11. Ya. B. Zel'dovich and Yu. P. Raizer, Physics of Shock Waves and High Temperature Hydrodynamic Phenomena , Academic Press.
12. E. Cnare, "Magnetic flux compression by magnetically imploded metallic foils," J. Appl. Phys., 37, No. 10 (1966).
13. V. T. Mikhkel'soo, G. A. Shneerson, and A. P. Shcherbakov, "The production of a superstrong magnetic field by the capture and compression of flux by a short cylindrical shell," Prib. Tekh. Eksp., No. 2 (1974).
14. N. B. Volkov, V. T. Mikhkel'soo, E. N. Nagel', and G. A. Shneerson, "A numerical investigation of magnetodynamic cumulation," Energet. Transport, Izv. Akad. Nauk SSSR, No. 6 (1976).
15. V. T. Mikhkel'soo, "An investigation of the magnetic field of a massive solenoid with a thin-walled shell," in: Electromagnetic Processes in Power Equipment [in Russian], Leningrad Polytechnic Inst. (1971).
16. N. V. Volkov, "Numerical solution of the magnetohydrodynamic problem on the compression of magnetic flux by a conducting shell," Vestn. KhPI, No. 123, Issue 4 (1977).
17. J. P. Somon, "The equation of state of a solid," LGI Report No. 64/3 (1964).
18. S. B. Kormer, A. I. Funtikov, et al., "Dynamic compression of porous metals and the equation of state with variable specific heat at high temperatures," Zh. Eksp. Teor. Fiz., 42, 686 (1962).
19. L. D. Landau and E. M. Lifshits, Statistical Physics [in Russian], Nauka, Moscow (1976).

20. L. I. Sedov, The Mechanics of Continuous Media [in Russian], Vol. 1, Nauka, Moscow (1976).
21. H. Knoepfel and R. Luppi, "The electrical conductivity of metals at very high temperatures," in: Exploding Wires, Vol. 4, London (1968), p. 233.
22. N. B. Volkov, "An investigation of electrophysical processes occurring in connection with the production of superstrong pulsed magnetic fields," Author's abstract of Candidate's Dissertation, Engineering Sciences, Leningrad Polytechnic Inst. (1978).
23. N. B. Volkov, "A plasma model of the conductivity of metals," Zh. Tekh. Fiz., 49, No. 9 (1979).
24. A. Brin, J. E. Besanson, et al., "Magnetic field compression," in: Proceedings of the Conference on Megagauss Magnetic Field Generation by Explosives and Related Experiments, Euratom, Brussels (1966).
25. C. M. Fowler, W. B. Garn, and R. S. Caird, "Production of very high magnetic fields by implosion," J. Appl. Phys., 31, 588 (1960).
26. A. D. Sakharov, R. Z. Lyudaev, et al., "Magnetic cumulation," Dokl. Akad. Nauk SSSR, 165, No. 1 (1965).
27. G. Lehner, J. G. Linhart, and J. P. Somon, "Limitations on magnetic fields obtained by flux compression," Nucl. Fusion, 4, 362 (1964).
28. F. Herlach, "Megagauss magnetic fields," Reports on Progress in Physics, 31, 341 (1968).
29. H. Knoepfel, Pulsed Magnetic Fields, Elsevier (1970).

POSSIBILITY OF APPLYING ELECTROMAGNETIC ACCELERATORS TO INVESTIGATE PROCESSES OCCURRING IN THE HIGH-VELOCITY COLLISION OF SOLIDS

V. F. Agarkov, A. A. Blokhintsev, S. A. Kalikhman, V. I. Kuznetsov, V. N. Fomakin, and A. A. Tsarev

UDC 538.323:534.2

Experiment on the high-velocity collision of structure specimens with particles of less than a millimeter in size at 1-15-km/sec speeds are necessary for the investigation of material properties by the application of mechanical forces. Promising accelerating apparatus are electromagnetic accelerators that use the powerful action of an electromagnetic field on conductors with current. It turns out to be possible to accelerate cylindrical conductors of less than 1-mm diameter to velocities exceeding 10 km/sec [1] in the regime of separate regulation of the accelerating magnetic field and the current in the conductor.

1. Quite important to the quantitative estimate of high-velocity action is the question of the size of the body being accelerated at the time of the collision. If the current density is less than the limit according to the fusion condition, and the conductor diameter is much less than the equivalent depth of penetration ($\Delta_e = \sqrt{2/\omega\sigma\mu_0}$, where ω is the circular frequency of the discharge current, and σ, μ_0 are the conductivity and magnetic permittivity of the conductor material), then sausage-type instabilities cannot develop [2] and the diameter can be considered constant. The length of the conductor diminishes because of thermal processes at the sites of arc contact with the current-carrying rails during the acceleration. Heating occurs by the current flowing in the conductor (volume source) and because of the heat flux from the electrical contact arc (surface source). An analysis (see Appendix) shows that the combined effect of the volume and surface sources is limited, in practice, to a layer of thickness $2\sqrt{at}$, where a is the coefficient of thermal diffusivity and t is the time. Outside this layer, heat transfer from the contact zone can be neglected and it can be considered that the heating occurs only because of the volume source. We use this assumption to compute the evaporation rate and the diminution rate of the length of the conductor being accelerated because of evaporation. The maximal acceleration time and the corresponding limit velocity according to the heating conditions are determined by the time the conductor achieves a certain minimal size according to the conditions of the experimental investigations. Therefore, the energy balance equation has the form

Kuibyshev and Cheboksary. Translated from Zhurnal Prikladnoi Mekhaniki i Tekhnicheskoi Fiziki, No. 5, pp. 26-31, September-October, 1982. Original article submitted September 2, 1981.

0021-8944/82/2305-0617$07.50